

Author Manuscript

This is the author manuscript accepted for publication and has undergone full peer review but has not been through the copyediting, typesetting, pagination and proofreading process, which may lead to differences between this version and the [Version of Record](#). Please cite this article as [doi: 10.1111/ZSC.12477](https://doi.org/10.1111/ZSC.12477)

This article is protected by copyright. All rights reserved

1 **Corresponding Author:** Richard Harrington, 21 Sachem Street, Room 356 Environmental
2 Science Center, Yale University, New Haven, CT, USA, 06511. Phone: 203-432-7168.
3 Email: richard.harrington @ yale.edu

4
5 **Title:** Phylogenomic resolution of the monotypic and enigmatic *Amarsipus*, the Bagless
6 Glassfish (Teleostei, Amarsipidae)

7
8 **Authors:** RICHARD C. HARRINGTON, MATT FRIEDMAN, MASAKI MIYA,
9 THOMAS J. NEAR, MATTHEW [A.](#) CAMPBELL.

10
11 **Running Title:** Phylogenomic resolution of Amarsipidae.
12 Harrington *et al.*

13
14
15
16
17
18
19
20
21
22
23
24
25
26
27
28
29
30

31 **Abstract:**

32 *Amarsipus carlsbergi* is a rare mesopelagic fish distributed in the Indian and Pacific
 33 Oceans, and is the only species classified in the family Amarsipidae. Since its description in
 34 1969, phylogenetic hypotheses have varied regarding its relationship with other
 35 percomorph lineages, but most have indicated a close relationship with the traditional
 36 suborder Stromateoidei. Molecular phylogenies place families previously classified in
 37 Stromateoidei within a diverse clade—Pelagiaria— that includes fishes such as tunas,
 38 cutlassfishes, and pomfrets. A recent analysis of a small number of loci resolved a clade
 39 containing *Amarsipus* and the stromateoid lineage *Tetragonurus*. A subsequent high-
 40 throughput sequence phylogeny based on ultraconserved elements (UCEs) of Pelagiaria
 41 lacked *Amarsipus*, but revealed both strong support for stromateoid paraphyly and high
 42 levels of gene tree incongruence. We gathered UCE sequence data for 610 UCE loci from
 43 *Amarsipus* and integrate these with samples from all remaining pelagiarian families. This
 44 provides a taxonomically comprehensive phylogenomic framework to test the evolutionary
 45 relationships of *Amarsipus*, and evaluate the support for stromateoid monophyly. As in
 46 previous studies, our analyses find high levels of gene tree topological discordance with
 47 regard to some deeper pelagiarian inter-relationships. However, we resolve *Amarsipus* as
 48 the sister lineage of a clade containing *Tetragonurus* and a family not considered a
 49 stromateoid lineage, Chiasmodontidae. This relationship is supported by both high gene
 50 tree concordance and node support. Our analyses also provide strong support for the
 51 paraphyly of Stromateoidei, casting uncertainty on previous hypotheses of the evolution of
 52 morphological traits across members of Pelagiaria.

Deleted: hypotheses

Deleted: However, molecular

Deleted: phylogenetic analyses do not support monophyly of Stromateoidei. Instead, molecular phylogenies resolve some families previously classified in Stromateoidei as being most closely related to non-stromateoid lineages in a more inclusive clade Pelagiaria that include fishes such as tunas, cutlassfishes, and pomfrets.

Deleted: nuclear

Deleted: in order to provide a

Deleted: O

Deleted: , as well as

Deleted: .

74 **Introduction**

75

76 Acanthomorph (spiny rayed) fishes represent an exceptionally diverse clade that
 77 comprise more than 19,000 species and 320 families (Fricke, Eschmeyer, & van der Laan,
 78 2020), and pose many challenges for ichthyologists interested in their phylogenetic
 79 relationships. While acanthomorph phylogenetic uncertainty spans both ancient and more
 80 recent divergences, some of the most pernicious challenges involve the resolution of deep
 81 interrelationships where identification of shared derived morphological features among
 82 lineages with long, independent evolutionary histories can be difficult (Johnson, 1993;
 83 Nelson, et al., 2016; Girard et al., 2020). The **application** of molecular **phylogenetics** has
 84 advanced many aspects of our understanding of acanthomorph relationships (e.g., Near et
 85 al., 2013; Betancur-R et al., 2013; Thacker et al., 2015; Alfaro et al., 2018; Hughes et al.,
 86 2018), but it has also highlighted challenging areas where evolutionary phenomena such as
 87 incomplete lineage sorting (ILS) or limited phylogenetic informativeness pose barriers to
 88 phylogenetic analysis with relatively small numbers of loci (Harrington et al., 2016). This
 89 challenge is conspicuous for Pelagiaria, an acanthomorph subclade of mostly pelagic, open-
 90 ocean fishes that includes some of the most extensively studied species from a
 91 morphological standpoint (e.g., Scombridae, the tunas and mackerels) as well as less
 92 familiar and deep-sea lineages (e.g., the Ragfish, *Icosteus aenigmaticus* and swallows of
 93 the family Chiasmodontidae). Our understanding of the interrelationships among
 94 pelagiarian families remains clouded by numerous opposing systematic hypotheses
 95 informed by either morphological or molecular data.

Deleted: rapidly expanding field

Deleted: phylogenetics

96 Hints that the morphologically disparate lineages comprising Pelagiaria share
 97 common ancestry appeared in several early molecular phylogenetic studies that lacked
 98 consistent taxonomic coverage of pelagiarian lineages (e.g., Chen et al., 2003; Smith &
 99 Craig, 2007; Yagashita et al., 2009). A mitogenomic study by Miya et al. (2013) provided
 100 the first comprehensive synthesis that included nearly all relevant families and defined
 101 Pelagiaria as a clade, uniting sixteen families previously classified among six different
 102 percomorph suborders. Christened Pelagia by Miya et al. (2013), the clade included
 103 members of two fixtures of 20th century acanthomorph classifications: the Scombroidei

106 (Scombridae, Scombrolabracidae, Gempylidae, and Trichiuridae) and the Stromateoidei
 107 (Amarsipidae, Ariommatidae, Centrolophidae, Nomeidae, Stromateidae, and
 108 Tetragonuridae) (e.g., Regan, 1902; Greenwood, 1966; Johnson, 1984). The billfishes,
 109 Xiphiidae and Istiophoridae, long classified in Scombroidei, are resolved as distantly related
 110 to all other pelagarians in molecular phylogenies (e.g., Orell et al., 2006; Harrington et al.,
 111 2016; Alfaro et al., 2018; Hughes et al., 2018). Despite strong support for monophyly of
 112 Pelagiaria across diverse molecular phylogenetic studies, the monophyly of either the
 113 traditional Scombroidei or Stromateoidei as subgroups within Pelagiaria is not supported
 114 (Near et al., 2013; Betancur-R et al., 2013; Orrell et al., 2006; Little et al., 2010; Miya et al.,
 115 2013; Alfaro et al., 2018; Hughes et al., 2018; Friedman et al., 2019). The lack of support
 116 for stromateoid monophyly was an unanticipated result of molecular analyses due to the
 117 presence of a compelling morphological character shared among these fishes: the
 118 pharyngeal sac, a variously toothed sac-like structure located behind the gill arches, and
 119 hypothesized to facilitate the processing of gelatinous zooplankton such as jellyfish or salps
 120 that comprise the diet of many stromateoid species (Mansueti, 1963; Janssen & Harbison,
 121 1981).

122 *Amarsipus carlsbergi* (Fig. 1) is the only species in the family Amarsipidae and has
 123 been classified in Stromateoidei since its discovery and description (Haedrich, 1969).

124 Although *Amarsipus* lacks the pharyngeal sac that is typical of other stromateoids, this rare
 125 species from the Indo-Pacific was allied with the stromateoids on the basis of several
 126 morphological features thought to be typical for the group, but of questionable systematic
 127 value: uniserial teeth in the jaws, an expanded lacrimal bone, and an extensively developed
 128 subdermal canal system (Haedrich, 1969). Subsequent phylogenetic hypotheses based on
 129 morphology resolved *Amarsipus* as either sister to all stromateoids (e.g. Haedrich, 1971;
 130 Horn, 1984), nested within stromateoids (Doiuchi et al., 2004), or proposed that it is not
 131 even a member of the clade (Springer & Johnson, 2004) (Fig. 2). DNA samples for
 132 *Amarsipus* did not become available for molecular analyses until 2018, and phylogenetic
 133 analysis of several nuclear protein-coding loci and mitochondrial 16S RNA resolved
 134 *Amarsipus* and the stromateoid *Tetragonurus* as sister lineages (Campbell et al., 2018) (Fig.
 135 2). As in previous molecular analyses (Near et al., 2013; Betancur-R et al., 2013; Miya et

Deleted: io

Deleted: stromatioid

Deleted: described

Deleted: i

Deleted:

141 al., 2013), deeper nodes in Pelagiaria were poorly supported, and this molecular analysis
 142 did not resolve Stromateoidei as a monophyletic group.

143 A phylogenomic analysis of nearly 1000 ultra-conserved elements (UCEs) that
 144 included 15 of the 16 families of Pelagiaria, lacking only *Amarsipus*, revealed substantial
 145 gene tree discordance that hampered resolution of deeper nodes in the phylogeny (Friedman
 146 et al., 2019). This was reflected by incongruent phylogenetic trees resulting from different
 147 methods of phylogenetic inference. While the phylogenomic analyses resolved a **majority**
 148 **of stromateoid species in a** strongly supported ‘core’ clade that **contains** Ariommatidae,
 149 Nomeidae, and Stromateidae, the resolution of Centrolophidae and *Tetragonurus* in
 150 Pelagiaria rendered Stromateoidei polyphyletic with varying degrees of node support. The
 151 placement of Centrolophidae was variable and had low node support across species tree-
 152 and concatenation-based analyses. However, the UCE phylogenies consistently resolved
 153 with strong support a sister relationship between *Tetragonurus* and Chiasmodontidae, a
 154 family that lacks a pharyngeal sac and previously had not been hypothesized to belong to
 155 the stromateoid group.

156 The evolutionary history of *Amarsipus carlsbergi* is important in **evaluating the**
 157 phylogenetic relationships of Stromateoidei and is critical to the assessment of the
 158 evolution of the pharyngeal sac among lineages of Pelagiaria. With *Amarsipus* lacking in
 159 the analyses of Friedman et al. (2019), it remained unknown whether genomic-scale data
 160 would corroborate the relationship between *Amarsipus* and *Tetragonurus* as inferred with a
 161 smaller number of loci (Campbell et al., 2018), or if this putative stromateoid lineage would
 162 resolve in a group with core stromateoids or with other pelagiarian lineages. In this study,
 163 we assess the phylogenetic relationships of *Amarsipus carlsbergi* using an expanded UCE
 164 dataset that includes all families of Pelagiaria (Friedman et al., 2019).

165 **Methods**

166

167 *Generation of UCE Loci from Whole Genome Sequencing Data*

168

169 We extracted UCE sequences from paired-end Illumina sequence data obtained
 170 from a single individual of *Amarsipus carlsbergi* (CBM-ZF 17750; NCBI SRA

Deleted: stromateoid

Deleted: contains

Deleted:

Deleted: ,

Deleted: assessing

176 SRX4707127) that was previously analyzed in Campbell et al. (2018). Details on quality
 177 control protocols for the removal of low-quality bases, adapter contamination, and
 178 combination of overlapping paired-end reads can be found in Campbell et al. (2018). Post
 179 quality-control reads were mapped to reference assemblies resulting from target capture of
 180 UCEs from Friedman et al. (2019). [Museum voucher accession information, as well as](#)
 181 [NCBI Sequence Read Archive \(SRA\) BioProject and BioSample accession numbers for](#)
 182 [each specimen are provided in Supplemental Table 1.](#) We performed three mappings to
 183 different pelagiarian species in order to confirm the fidelity of *Amarsipus* UCE data. These
 184 replicates were mapped against *Icosteus aenigmaticus*, *Kali normani* and *Thunnus*
 185 *orientalis*, the three samples that had the highest overall completeness in the 95% complete
 186 dataset of Friedman et al. (2019). Mapping was conducted with Burrows-Wheeler Aligner
 187 (BWA) version 0.7.7-r441 using the MEM algorithm for both paired sequences and
 188 unpaired reads (Li & Durbin, 2009). The resulting Binary Alignment Map (BAM) files
 189 were processed with SAMTools version 1.3 (Li et al., 2009) to combine separate paired and
 190 unpaired BAM files and to filter for a minimum alignment score (MAPQ) of 30 (99.90%
 191 accuracy, -q 30). Consensus sequences for each UCE locus in the reference assembly were
 192 generated from the filtered BAM file with the proovread version 2.14 bam2cns subprogram
 193 (Hackl et al., 2014). The resulting consensus sequences were refined by removing bases
 194 with quality scores of less than 30 with seqtk version 1.3-r106
 195 (<https://github.com/lh3/seqtk>). Resulting consensus sequences were aligned to the 95%
 196 complete UCE matrix from Friedman et al. (2019) with MAFFT version 7.130B (Katoh et
 197 al., 2002; Katoh et al., 2013). Although the *T. orientalis* reference assembly had the third
 198 most UCEs (610), it presented the most assembled bases (346,792) and largest mean contig
 199 length (568.51). The *T. orientalis* assembly was selected for use in all downstream
 200 phylogenetic analyses, although preliminary phylogenies were inferred with all three
 201 assemblies in order to verify the equivalent phylogenetic position of the mapping.

202 *Phylogenetic Analyses*

203

204 We used both concatenated supermatrix and species tree approaches. [All](#)
 205 [phylogenies were inferred with a set of UCE loci that have 95% taxonomic completeness.](#)

Deleted: inferred phylogenies of *Amarsipus* and *Pelagiaria* using...

208 and all of which contain sequence data for *Amarsipus*. Although previous studies
209 demonstrated sensitivity of the deepest pelagiarian relationships to both the loci used and
210 data matrix completeness (e.g., Miya et al., 2013, Campbell et al., 2018, Friedman et al.,
211 2019), we restricted our analyses to this data matrix in order to reduce uncertainty in the
212 resolution of *Amarsipus* by the inclusion of loci that lack coverage for this species. For
213 analyses of concatenated data, we first determined partitioning schemes using
214 PartitionFinder2 v2.1.1 (Lanfear et al., 2016) using the relaxed hierarchical clustering
215 search algorithm (Lanfear et al., 2014) and Bayesian Information Criterion for partitioning
216 scheme selection, and a GTR-Gamma model of molecular evolution. We conducted
217 partitioned Bayesian tree inference using ExaBayes v1.5 (Aberer et al., 2014), with an
218 analysis consisting of 4 Markov chain Monte Carlo (MCMC) runs for 10 million
219 generations and trees and parameters sampled every 1000 generations. We discarded the
220 first 50% of sampled trees as burn-in, and summarized the consensus tree using the
221 Exabayes consens program. Topological convergence was assessed by ensuring that
222 average standard deviation of split frequencies was below 5%. To confirm convergence in
223 other parameter estimates, we used Tracer v1.7.1 (Rambaut et al., 2018), ensuring effective
224 sample sizes above 200 and no post-burnin directional trends in parameter traces. We also
225 performed a partitioned maximum likelihood tree search on the concatenated data matrix
226 using IQTree v 1.6.12 (Nguyen et al., 2015). This was conducted with the ultrafast
227 bootstrap approximation and nearest-neighbor interchange optimization (Hoang et al.,
228 2018) with 1000 bootstrap replicates.

229 We implemented a summary species tree inference with ASTRAL-III v5.6.3 (Zhang
230 et al., 2018), based on individual gene trees estimated for each UCE locus using IQTree v
231 1.6.12. For each locus, we determined the optimal model of molecular evolution using the
232 ModelFinder Plus (Kalyaanamoorthy et al., 2017) option within IQTree. Individual-locus
233 tree searches were conducted using Shimodaira-Hasegawa approximate likelihood ratio test
234 (SH-aLRT) with 1,000 bootstrap replicates. Summary species tree analyses may be
235 susceptible to influence from nodes that have marginal support within individual gene trees,
236 and contracting branches that subtend weakly supported partitions has been shown to
237 improve accuracy of species tree inference (Zhang et al., 2018). The relatively short UCE

238 loci in our analysis (average length of 672 base pairs, and 259 parsimony informative sites
239 per locus) may result in gene trees that contain low-support nodes among some taxa. In
240 order to assess the influence of low-support gene tree nodes on our species tree topology,
241 particularly with regard to the placement of *Amarsipus* and the status of stromateoid
242 monophyly, we generated a series of species trees using gene trees for which branches were
243 collapsed across a range of thresholds, corresponding to 15, 30, and 45% bootstrap support.

244 *Hypothesis Testing*

245

246 We examined evidence for three hypotheses present in the post-burnin tree sample
247 generated by ExaBayes as described in the previous section. The three hypotheses
248 evaluated were: (1) monophyly of Stromateoidei as classically recognized (e.g., Haedrich,
249 1969), (2) the presence of a clade comprising Amarsipidae, Tetragonuridae, and
250 Chiasmodontidae, and (3) monophyly of pelagiarians with a pharyngeal sac (i.e., classical
251 Stromateoidei excluding Amarsipidae). Trees from ExaBayes were imported into R version
252 3.6.1 with the `read.nexus` function of *ape* version 5.3. The number of times each hypothesis
253 was present in the post-burnin tree sample was calculated with the `is.monophyletic` function
254 of *ape* and the corresponding posterior probability generated by dividing this number by the
255 number of trees examined. We then calculated Bayes factors by dividing the posterior
256 probabilities of Stromateoidei monophyly and the monophyly of fishes with a pharyngeal
257 sac by the posterior probability of a clade composed of Amarsipidae, Tetragonuridae, and
258 Chiasmodontidae.

259 *Analysis of Concordance*

260

261 We used BUCKy (Ané et al., 2007) to analyze the topological concordance across
262 the set of gene trees inferred for each individual UCE locus. BUCKy summarizes the
263 occurrence of topological partitions in the posterior distribution of gene trees from each
264 loci's Bayesian gene tree search, and provides concordance factors, which are estimates of
265 the probability that any particular bipartition among taxa reflects the true topology of loci in
266 the dataset. For this analysis, we generated gene tree distributions using MrBayes v. 3.2.7
267 (Ronquist et al., 2012). In each MrBayes analysis, we ran four MCMC chains of 2 million

268 generations in length, with a sampling frequency of 2000 generations, and a GTR-Gamma
269 model of molecular evolution. Using the BUCKy program mbsum, branching patterns
270 within each loci's posterior tree distribution were summarized, excluding the first 75% of
271 the distribution as burn-in. Increases in the number of species in a phylogeny result in non-
272 linear increases in possible topologies, which can be computationally intractable for
273 BUCKy when dealing with large taxonomic datasets. To reduce the computational burden
274 of summarizing partition patterns across our dataset, we conducted our BUCKy
275 concordance factors analysis using a single representative of each of the 16 pelagiarian
276 families, selecting individuals from each family with the highest representation in the UCE
277 gene trees ([Supplemental Table 2](#)). We estimated concordance factors in BUCKy using an
278 alpha level (prior parameter for expectation of locus linkage across the dataset) of 1.0, but
279 also compared concordance values when alpha was set to 0.75 and 0.5.

280 While BUCKy concordance factors provide a convenient method to assess the
281 topological agreement across a multi-locus dataset, they do not explicitly reveal the node
282 support from individual loci in the dataset. We used the program Phyparts (Smith et al.,
283 2015) to summarize the statistical node support from individual UCE gene trees in our
284 dataset. Given a reference tree topology for a set of taxa (e.g, our ASTRAL-III species tree
285 or ExaBayes concatenated tree) and a set of gene trees, Phyparts summarizes the number of
286 loci for which a node in the reference tree receives strong support, as well as the number of
287 loci that strongly support alternative topologies or are uninformative to a particular
288 relationship. For the Phyparts summary analysis, we used the IQTree-inferred gene trees
289 generated for our species tree analyses (described above). As in BUCKy concordance
290 factors analyses, we reduced computational burden of examining partition variation across
291 many taxa by pruning our reference trees and individual UCE locus trees to a set of 42 taxa,
292 with two representatives per family (unless the family is monotypic or for which we had
293 only a single representative) ([Supplemental Table 3](#)). This allowed us to summarize support
294 for relationships among major pelagiarian lineages without attempting to summarize
295 support for intrafamilial variation. We estimated support for partitions that occurred in our
296 ASTRAL-III and concatenated IQTree analyses, with bootstrap support observed in
297 individual UCE gene trees of 50 or 80 as the 'significant' threshold. While bootstrap values

298 of 50 or 80 are not traditionally considered especially strong support in molecular gene
299 trees, we were interested in the relative number of loci that exceed these thresholds for
300 competing alternative relationships.

301 Results

302

303 *Alignment of reads and UCE sequence generation*

304

305 After filtering for a minimum alignment quality score ($\text{MAPQ} \geq 30$), 123,054 of the
306 258,232,994 paired reads and 80,050 of the 181,354,946 unpaired reads present after initial
307 quality control processing aligned to the *Thunnus orientalis* reference UCES. The resulting
308 average per-site coverage across reference *Thunnus orientalis* UCES is 30.13. After
309 removing bases with a quality score of less than 30, the consensus sequences contained
310 337,705 bases with an average length of 553.61 across 610 UCE loci. After alignment with
311 all samples, total length of the concatenated 610 UCE locus dataset is 410,063 base pairs,
312 with a mean of 672 base pairs per individual locus.

313 *UCE placement of Amarsipus and relationship of stromateoid families*

314

315 The topology inferred from the concatenated, partitioned 610 UCE locus dataset is
316 identical between the Exabayes and IQTree analyses, and patterns of Bayesian posterior
317 probability (BPP) and maximum likelihood bootstrap (BS) node support are also highly
318 similar between analyses (Fig. 3). *Amarsipus* was inferred as sister to a clade containing
319 *Tetragonurus* and Chiasmodontidae with maximum node support (BPP of 1.0; BS of 100),
320 as was the sister relationship between *Tetragonurus* and Chiasmodontidae. This clade
321 containing *Amarsipus*, *Tetragonurus*, and Chiasmodontidae is resolved as sister to
322 Scombridae with strong support (BPP 1.0; BS 96). Other aspects of this topology that are
323 strongly supported and are similar to what was reported in Friedman et al. (2019), and
324 include: a sister-group relationship between Bramidae and Caristiidae; a clade containing
325 *Scombrobrax*, Gempylidae, and Trichiuridae; and a 'core stromateoid' clade that contains
326 Ariommatidae, Nomeidae, and Stromateidae. As in Friedman et al. (2019), Gempylidae
327 was rendered paraphyletic due to the placement of *Lepidocybium*, which is sister to a

Deleted: was

329 lineage containing the remainder of Gempylidae and Trichiuridae. The primary differences
 330 between our topology and that of Friedman et al. (2019) involve the families identified by
 331 those authors as ‘rogue’ taxa: *Arripidae*, *Icosteus*, *Centrolophidae*, and *Pomatomus*. These,
 332 were shown to be highly sensitive to analytical framework or data filtering approach. While
 333 our concatenated analyses find strong support for a clade uniting *Pomatomus* and
 334 *Centrolophidae* (BPP 1.0; BS 95), the nodes subtending its relationship to ‘core
 335 stromateoids’ and the remaining pelagiarian families— particularly *Arripidae* and *Icosteus*—
 336 all received relatively low support.

337 Our series of ASTRAL-III species tree analyses resulted in two topologies that
 338 correspond to whether or not the input gene trees were subjected to branch contraction at
 339 various thresholds of node bootstrap support (Fig. 4). The topology of species trees whose
 340 gene trees’ branches were collapsed for nodes not exceeding 15, 30, or 45% BS, all
 341 converged on an identical topology, and ASTRAL-III’s metric of node support (local
 342 posterior probability [LPP]) differed slightly among these replicates. We present the tree
 343 and node support from the 15% threshold of node contraction in Figure 2C. Across all
 344 species tree analyses, *Amarsipus* was inferred as sister to a clade including *Tetragonurus*
 345 and Chiasmodontidae with strong LPP support (Fig. 4). As in the concatenated analysis, we
 346 also observed consistently high support for a *Scombrobrax*-gempylid-trichiurid clade and
 347 a ‘core stromateoid’ clade, which appeared in each of the replicate ASTRAL-III analyses.
 348 A primary difference is that the node-collapsed species trees find *Icosteus* is sister to a
 349 clade containing *Pomatomus* + *Centrolophiidae* and ‘core stromateoids’, and this entire
 350 group sister to a clade containing *Arripidae* and *Scombridae*. In the species tree generated
 351 without filtering based on node bootstrap support, *Scombridae* is sister to the clade
 352 *Amarsipus* + *Tetragonurus* + Chiasmodontidae, which is similar to the topology from
 353 concatenation analyses.

354 Examination of the posterior tree distribution of the concatenated ExaBayes analysis
 355 reveals that the clade comprising *Amarsipus*, *Tetragonurus*, and Chiasmodontidae was
 356 present in all posterior trees examined (BPP = 1.00). The resulting Bayes factors, which
 357 consider the monophyly of Stromateoidei (BPP=0.00, Bayes factor = 0.00/1.00 = 0.00) and
 358 the monophyly of fishes with a pharyngeal sac (BPP=0.00, Bayes factor = 0.00/1.00 =

- Deleted: ,
- Deleted: which
- Deleted: shown
- Deleted: and which included *Arripidae*, *Icosteus*, *Centrolophidae*, and *Pomatomus*
- Deleted: Stromateoids’

365 0.00), strongly support the clade comprising *Amarsipus*, *Tetragonurus*, and
 366 Chiasmodontidae.

367 *Concordance of Loci, and measures of UCE support*

368

369 The close relationship between *Amarsipus*, *Tetragonurus*, and Chiasmodontidae is
 370 supported by relatively high sample-wide concordance among topologies of individual
 371 UCE gene trees. A partition containing these three taxa occurs in 44.8% of loci (95% CI:
 372 42.3-47.3%) (Fig. 5, Table 1). The interrelationships between these three lineages exhibit a
 373 moderate level of discordance, with similar percentages of loci inferring the three
 374 alternative topologies and with overlapping 95% credible intervals. In our dataset, a sister
 375 relationship between *Tetragonurus* and Chiasmodontidae, to the exclusion of *Amarsipus*, is
 376 present in 25.5% [95% CI: 22.3-28.8%] of loci. The alternative topologies, where
 377 *Amarsipus* occurs in a partition with either *Tetragonurus* or Chiasmodontidae, to the
 378 exclusion of the other, occur in 20.1% [95% CI: 16.9-23.4%] and 19.4% [95% CI: 16.4-
 379 22.6%] of loci, respectively. By contrast, the percentage of loci for which *Amarsipus* occurs
 380 in a partition with any of the other individual families of Pelagiaria is substantially lower,
 381 ranging between 0.9 to 3.5% (Fig. 5).

382 In contrast to the similar concordance factors estimated for gene tree topologies that
 383 are nearly equally divided between the three alternative sets of relationships among
 384 *Amarsipus*, *Tetragonurus*, and Chiasmodontidae (with the highest number resolving
 385 *Tetragonurus* + Chiasmodontidae), only the clade uniting *Tetragonurus* and
 386 Chiasmodontidae receives strong bootstrap support in more than a handful of individual
 387 UCE gene trees. A sister relationship between these two lineages, to the exclusion of
 388 *Amarsipus*, meets the threshold of 50% and 80% bootstrap support in 91 (15% of loci) and
 389 38 (6% of loci) gene trees, respectively (Table 1). A sister relationship between *Amarsipus*
 390 and *Tetragonurus* meets the 50% bootstrap support in 4 gene trees, and 80% in one 1 tree
 391 (0.7% and 0.1% of loci, respectively). Similarly, only 4 gene trees have at least 50%
 392 bootstrap support for a sister relationship between *Amarsipus* and Chiasmodontidae, with
 393 only a single of these loci surpassing the 80% bootstrap threshold (representing 0.7% for
 394 BS of 50, and 0.1% of loci for BS of 80).

Deleted: monophyly of

Deleted: 4

397 Patterns of sample-wide topological concordance among the remaining pelagiarian
 398 families are similar to those reported in Friedman et al. (2019). For instance, our dataset has
 399 a relatively high frequency of occurrence for partitions that include Trichiuridae and
 400 Gempylidae (50.7% [95CI: 48.1-53.5], versus 48.2% [95CI: 45.8-51.0] in Friedman et al.
 401 (2019)) and Ariommatidae-Nomeidae (45.1% [95CI: 42.3-47.8], versus 44.5% [95CI: 42.0-
 402 47.2] in Friedman et al. (2019)). The ‘rogue’ lineages of Arripidae, *Icosteus*,
 403 Centrolophidae, and Pomatomidae appeared in partitions with overlapping 95% confidence
 404 intervals with at least 7 of other pelagiarian families. For example, concordance estimates
 405 for a partition containing Arripidae and each of nine other pelagiarian families have
 406 overlapping 95% credible intervals, ranging between 3.1 - 6.7% of loci containing these
 407 alternative relationships. Scombridae, which in all of our molecular phylogenetic analyses
 408 is resolved as a sister lineage of a clade containing *Amarsipus*, *Tetragonurus*, and
 409 Chiasmodontidae (but with only modest support), has concordance factors with overlapping
 410 95% credible intervals for eight pelagiarian families.

411 A clade composed of only the families traditionally classified as belonging to
 412 Stromateoidei appears in the MrBayes-generated posterior tree distributions of three UCE
 413 loci, although at a frequency low enough such that BUCKy estimates a probability that it
 414 reflects the true topology of none of these loci (concordance factor of 0.00 [95% CI = 0.0-
 415 0.003]). A clade containing all traditional stromateoid families plus Chiasmodontidae, to
 416 the exclusion of all other pelagiarian families, receives only a slightly higher concordance
 417 factor of 0.003 [95% CI = 0.0-0.008], occurring in the posterior distribution of 8 loci, and
 418 has a 0.975 probability of representing the true topology of only three loci. Likewise, a
 419 clade that includes only the stromateoid lineages that are known to have pharyngeal sacs
 420 (i.e., *Tetragonurus*, Ariommatidae, Centrolophidae, Nomeidae, and Stromateidae) receives
 421 a concordance factor estimate of 0.00.

422 Discussion

423

424 This study provides the first genomic-scale analysis of the phylogenetic
 425 relationships of *Amarsipus*, and the second molecular study to contain sufficient taxonomic
 426 sampling of Pelagiaria to evaluate the relationships of taxonomic families classified in the

Deleted: presents

428 Stromateoidei. We present several phylogenies inferred using concatenation and coalescent
429 species tree summary methods (Figs 3 and 4), and explore concordance among loci to
430 highlight confidence for a clade containing *Amarsipus*, *Tetragonurus*, and
431 Chiasmodontidae. The rapid increase in high-throughput sequencing for phylogenetic
432 analyses has sparked debate about the most appropriate approaches for tree inference and
433 interpretation of node support with large, genomic-scale datasets (e.g., Gatesy & Springer,
434 2014; Mendes & Hahn, 2018; Gatesy et al., 2019). Although coalescent species tree
435 analyses attempt to model the independent evolutionary history of many unlinked loci,
436 species tree accuracy is affected by high levels of ILS or erroneous gene tree inference–
437 phenomena that can be exacerbated by ‘anomaly zone’ scenarios of rapid, deep divergences
438 (Degnan & Rosenberg, 2006; Walker et al., 2018; Gatesy et al., 2019). Fossil-calibrated
439 divergence time estimates from [Alfaro et al. \(2018\)](#) and [Friedman et al. \(2019\)](#) support a
440 scenario of rapid diversification of major pelagiarian lineages beginning around the
441 Cretaceous-Paleogene boundary (66 million years ago) and extending through the
442 Paleocene. A series of rapid, successive divergence events among major lineages early in
443 pelagiarian history create a phylogenetic scenario that is difficult to resolve with the simple
444 addition of more loci and analyzed in traditional concatenated or coalescent species tree
445 analytical frameworks (e.g., Campbell et al., 2017; Campbell et al., 2020). This is reflected
446 in the relatively high levels of gene tree discordance, low node support, and inferred
447 topologies that are inconsistent with regard to the relationships among the oldest nodes
448 within the pelagiarian phylogeny (Fig 2).

449 Campbell et al. (2018) provided the first molecular phylogenetic study of
450 *Amarsipus*, which resolved it and *Tetragonurus* as sister lineages as well as non-monophyly
451 of the Stromateoidei. The subsequent study by [Friedman et al. \(2019\)](#) investigated the
452 relationships of Pelagiaria with a phylogenomic analysis utilizing nearly 1000 UCE loci,
453 and identified several ‘rogue’ lineages (e.g., Arripidae, *Icosteus*, and *Pomatomus*) due to
454 the prevalence of discordant UCE gene tree topologies that resulted in their variable and
455 weakly supported phylogenetic resolution across analyses. However, [Friedman et al. \(2019\)](#)
456 did not include *Amarsipus* in their phylogenomic analyses.

Deleted: *i*

458 The phylogenomic analysis of UCE data demonstrates that the phylogenetic
 459 resolution of *Amarsipus* as the sister lineage of a clade containing *Tetragonurus* and
 460 Chiasmodontidae is one of the most robustly supported relationships among major
 461 pelagiarian lineages by metrics of node support and gene tree topological concordance
 462 (Figs 3, 4, and 5). Thus, *Amarsipus* is not a ‘rogue’ lineage. While the topologies of
 463 individual UCE loci in our dataset contain partitions for each of the three possible
 464 relationships among *Amarsipus*, *Tetragonurus*, and Chiasmodontidae at nearly equal
 465 frequency, the only topology that garnered strong bootstrap support from more than four
 466 loci was the sister relationship between *Tetragonurus* and Chiasmodontidae, which had
 467 bootstrap support greater than 50% in 91 loci (Table 1). This asymmetry between the nearly
 468 equal frequency of these alternative topologies versus disproportionate number of these
 469 gene trees inferred with strong support for a partition containing *Tetragonurus* and
 470 Chiasmodontidae may reflect that these two lineages have a longer, shared evolutionary
 471 history relative to *Amarsipus*, during which they would have accumulated concordant
 472 mutations that increase gene tree node support metrics. Among the remaining stromateoid
 473 lineages, the core clade of Ariommatidae, Nomeidae, and Stromateidae also receives
 474 consistent and strong molecular support (Campbell et al., 2018; Friedman et al., 2019).
 475 While across the more inclusive pelagiarian clade some relationships may remain
 476 unresolved, the phylogenetic resolution of *Amarsipus* and the non-monophyly of
 477 Stromateoidei are strongly supported in the phylogenomic analyses.

478 Previous phylogenetic analyses of morphological data resulted in different
 479 hypotheses regarding relationships of *Amarsipus* and the remaining stromateoid lineages.
 480 Haedrich (1969) and Horn (1984) hypothesized that *Amarsipus* is sister to all remaining
 481 stromateoids, a relationship that is consistent with a single origin of the modified
 482 stromateoid pharyngeal sac (Fig. 2A). Doiuchi et al. (2004) analyzed a larger
 483 morphological dataset (36 characters, rather than the 27 considered in Horn’s 1984 study)
 484 and concluded that *Amarsipus* was nested within the stromateoids and represented a
 485 secondary loss of the pharyngeal sac (Fig 2B). As with the early molecular phylogenetic
 486 studies of Pelagiaria, an unforeseen but key weakness of these morphological analyses was
 487 insufficient taxonomic coverage of non-stromateoid pelagiarian lineages, and only Doiuchi

Deleted: 1

Deleted: and

Deleted: 2

Deleted: , and thus,

Deleted: share a longer unique

Deleted: t

Deleted: analyzed

Deleted: Doiuchi

496 et al. (2004) included one such representative, *Arripis*. Regardless of their lack of broader
 497 sampling within Pelagiaria, none of the previous morphological hypotheses are congruent
 498 with our UCE-based results in which the six families traditionally classified as stromateoids
 499 represent a polyphyletic group that variously share most recent common ancestry with
 500 *Arripidae*, Icosteidae, Pomatomidae, Scombridae, and perhaps the all other lineages of
 501 Pelagiaria (Figs 3 and 4).

502 In contrast to the historical uncertainty regarding the position of *Amarsipus* among
 503 acanthomorph fishes, our analysis of UCE loci provides clear support for a close
 504 relationship between *Amarsipus*, *Tetragonurus*, and Chiasmodontidae and the non-
 505 monophyly of the traditional suborder Stromateoidei. The striking ecological and
 506 anatomical differences within the clade comprising *Tetragonurus* and Chiasmodontidae has
 507 been noted previously (Freidman et al., 2019), and resolution of *Amarsipus* as the sister
 508 lineage to this group only amplifies these contrasts. Unfortunately, our analyses do not
 509 resolve all of the backbone of pelagarian phylogeny, and there is phylogenetic uncertainty
 510 regarding the sister lineage of the strongly supported clade uniting *Amarsipus*,
 511 *Tetragonurus*, and Chiasmodontidae. The pharyngeal sacs that are a feature of five of the
 512 six stromateoid families have a long history of being interpreted as evidence of shared
 513 evolutionary history among these lineages (Haedrich, 1971; Horn, 1984; Doiuchi et al.,
 514 2004). Strong support for the clade containing *Amarsipus*, *Tetragonurus*, and
 515 Chiasmodontidae, and the associated non-monophyly of stromateoids highlights a more
 516 complicated evolutionary history of the pharyngeal sac. Although multiple losses or origins
 517 of the pharyngeal sac (and other morphological features of stromateoids) were
 518 unanticipated prior to the application of molecular phylogenetics, the lack of thorough
 519 taxonomic coverage in comparative morphological studies of pelagarian lineages has left a
 520 gap in our understanding of the origin of these key morphological traits. This gap in
 521 comparative morphological examination of Pelagiaria remains, but represents an important
 522 area of inquiry for advancing the understanding of pelagarian relationships. With modest
 523 diversity, mature genomic resources, and many anatomically well-documented lineages,
 524 Pelagiaria is an ideal candidate for integrative studies that seek to reconcile the contrasting
 525 phylogenetic signals of morphological and molecular datasets (e.g., Girard et al., 2020).

Deleted: *Arripus*Deleted: *Arripus*

Deleted:

Deleted: 1

Deleted: 2

Deleted: history in the evolution

Deleted: While

Deleted: direction in

534

535 **Data Availability**

536

537 Raw read sequence data for *Amarsipus carlsbergi* is available from the NCBI Sequence
 538 Read Archive (SRX4707127). UCE raw read data from Friedman et al. (2019) are available
 539 on the NCBI Sequence Read Archive under BioProject number PRJNA561597.

540 Alignments, individual UCE locus gene trees, and multi-locus phylogenies generated in this
 541 study are deposited in the Dryad Digital Repository (*doi link to be provided*).

542 **Acknowledgements**

543

544 The authors would like to thank Linda Ianniello (<https://lindaiphotography.com>) for
 545 providing digital images of *Amarsipus*; Makoto Okamoto (Marine Fisheries Research and
 546 Development Center, Fisheries Research Agency, Japan) for assistance with fish
 547 identification; and two anonymous reviewers for helpful comments on this manuscript.

548 **References**

549

550 Aberer, A.J., K. Kobert, & A. Stamatakis. 2014. ExaBayes: Massively parallel Bayesian
 551 tree inference for the whole-genome era. *Molecular Biology and Evolution* 31: 2553-2556.
 552 <https://doi.org/10.1093/molbev/msu236>.

553

554 Alfaro, M.E., Faircloth, B.C., Harrington, R.C., Sorenson, L., Friedman, M., Thacker, C.E.,
 555 Oliveros, C.H., Černý, D. & Near, T.J. 2018 Explosive diversification of marine fishes at
 556 the Cretaceous-Paleogene boundary. *Nature Ecology & Evolution* 2, 688-696.
 557 <https://doi.org/10.1038/s41559-018-0494-6>

558

559 Ané, C., Larget, B., Baum, D.A., Smith, S.D. & Rokas, A. 2007 Bayesian estimation of
 560 concordance among gene trees. *Molecular Biology and Evolution* 24, 412-426.
 561 <https://doi.org/10.1093/molbev/msl170>

562

Formatted: Default Paragraph Font, Font: (Default) +Body (Calibri), Font color: Black

Formatted: Font: Not Bold

563 Betancur-R., R., Broughton, R.E., Wiley, E.O., Carpenter, K., López, J.A., Li, C., Holcroft,
 564 N.I., Arcila, D., Sanciangco, M., Cureton, J.C., II, Zhang, F., Buser, T., Campbell, M.C.,
 565 Ballesteros, J.A., Roa-Varon, A., Willis, S., Borden, W.C., Rowley, T., Reneau, P.C.,
 566 Hough, D.J., Lu, G., Grande, T., Arratia, G., & Ortí, G. 2013 The tree of life and a new
 567 classification of bony fishes. *PLOS Currents* 5,
 568 ecurrents.tol.53ba26640df26640cace26675bb26165c26648c26288.
 569 <https://doi.org/10.1371/currents.tol.53ba26640df0cace26675bb165c8c26288>

570

571 [Campbell, M.A., Alfaro, M.E., Belasco, M., López, J.A. 2017. Early-branching euteleost](#)
 572 [relationships: areas of congruence between concatenation and coalescent model](#)
 573 [inferences. PeerJ 5:e3548 https://doi.org/10.7717/peerj.3548](#)

574

575 Campbell, M.A., Sado, T., Shinzato, C., Koyanagi, R., Okamoto, & M., Miya, M., 2018.
 576 Multilocus phylogenetic analysis of the first molecular data from the rare and monotypic
 577 Amarsipidae places the family within the Pelagia and highlights limitations of existing data
 578 sets in resolving pelagian interrelationships. *Molecular Phylogenetics and Evolution* 172–
 579 180. <https://doi.org/10.1016/j.ympev.2005.10.007>

580

581 [Campbell, M.A., Buser, T.J., Alfaro, M.E., López, J.A. 2020. Addressing incomplete](#)
 582 [lineage sorting and paralogy in the inference of uncertain salmonid phylogenetic](#)
 583 [relationships. PeerJ. 8:e9389. https://doi.org/10.7717/peerj.9389](#)

584

585 Chen, W.-J., Bonillo, C., & Lecointre, G. 2003. Repeatability of clades as a criterion of
 586 reliability: a case study for molecular phylogeny of Acanthomorpha (Teleostei) with larger
 587 number of taxa. *Molecular Phylogenetics and Evolution* 26, 262–288.
 588 [https://doi.org/10.1016/S1055-7903\(02\)00371-8](https://doi.org/10.1016/S1055-7903(02)00371-8)

589

590 Doiuchi, R., Tomoyasu, S., & Nakabo, T. 2004. Phylogenetic relationships of the
 591 stromateoid fishes (Perciformes). *Ichthyological Research* 51: 202-212.

592

Formatted: Default Paragraph Font, Font: (Default) +Body (Calibri), Font color: Text 1, English (UK)

Formatted: English (US)

- 593 Fricke, R., Eschmeyer, W. N., & van der Laan, R. (eds) 2020. Eschmeyer's Catalog of
 594 Fishes: Genera, Species, References.
 595 (<http://researcharchive.calacademy.org/research/ichthyology/catalog/fishcatmain.asp>).
 596 Electronic version accessed 25 August 2020.
 597
- 598 Friedman, M., Feilich, K.L., Beckett, H.T., Alfaro, M.E., Faircloth, B.C., Černý, D., Miya,
 599 M., Near, T.J., & Harrington, R.C. 2019. A phylogenomic framework for pelagiarian fishes
 600 (Acanthomorpha: Percomorpha) highlights mosaic radiation in the open ocean.
 601 *Proceedings of the Royal Society B* 286: 2091502. <https://doi.org/10.1098/rspb.2019.1502>
- 602
- 603 Gatesy, J., & Springer, M.S. 2014. Phylogenetic analysis at deep timescales: unreliable
 604 gene trees, bypassed hidden support, and the coalescent/concatenation conundrum.
 605 *Molecular Phylogenetics and Evolution* 80: 231-266.
 606 <https://doi.org/10.1016/j.ympev.2014.08.013>
- 607
- 608 Gatesy, J., Sloan, D.B., Warren, J.M., Baker, R.H., Simmons, M.P., Springer, M.S. 2019.
 609 Partitioned coalescence support reveals biases in species-tree methods and detects gene
 610 trees that determine phylogenomic conflicts. *Molecular Phylogenetics and Evolution* 139:
 611 <https://doi.org/10.1016/j.ympev.2019.106539>
- 612
- 613 Girard, M.G., Davis, M.P. and Smith, W.L. 2020. The Phylogeny of Carangiform Fishes:
 614 Morphological and Genomic Investigations of a New Fish Clade. *Copeia*, 108(2), pp.265-
 615 298. <https://doi.org/10.1643/CI-19-320>
- 616
- 617 Hackl, T., Hedrich, R., Schultz, J., Förster, F., 2014. proovread : large-scale high-accuracy
 618 PacBio correction through iterative short read consensus. *Bioinformatics* 30, 3004–3011.
 619 <https://doi.org/10.1093/bioinformatics/btu392>
- 620
- 621 Haedrich, R.L. 1967. The ~~stromateoid~~ fishes: systematics and classification. *Bulletin of the*
 622 *Museum of Comparative Zoology at Harvard College* 135: 31-139.

Formatted: Line spacing: 1.5 lines

Formatted: Default Paragraph Font, Font: (Default) Times New Roman, 12 pt, Font color: Auto

Deleted: stromateoid

- 624
625 Horn, M.H. 1984. Stromateoidei: Development and relationships. In: Richards, W.J.,
626 Cohen, D.M., Fahay, M.P., Kendall, A.W., & Richardson, S.L. (Eds). *Ontogeny and*
627 *Systematics of Fishes*. Special Publication. American Society of Ichthyologists and
628 Herpetologists, Lawrence, Kansas, pp. 620-628.
- 629
630 Harrington, R.C., Faircloth, B.C., Eytan, R.I., Smith, W.L., Near, T.J., Alfaro, M.E. &
631 Friedman, M. 2016. Phylogenomic analysis of carangimorph fishes reveals flatfish
632 asymmetry arose in a blink of the evolutionary eye. *BMC Evolutionary Biology* 16, 224.
633 <https://doi.org/10.1186/s12862-016-0786-x>
- 634
635 Hoang, D.T., Chernomor, O., von Haeseler, A., Minh, B.Q., & Vinh, L.S. 2018. UFBoot2:
636 Improving the ultrafast bootstrap approximation. *Molecular Biology and Evolution*
637 35:518–522. <https://doi.org/10.1093/molbev/msx281>
- 638
639 Hughes, L., Ortí, G., Huang, Y., Sun, Y., Baldwin, C., Thompson, A.W., Arcila, D.,
640 Betancur-R., R., Li, C., Becker, L., Bellora, N., Zhao, X., Li, X., Wang, M., Fang, C., Xie,
641 B., Zhou, Z., Huang, H., Chen, S., Venkatesh, B., & Shi, Q. 2018 Comprehensive
642 phylogeny of ray-finned fishes (Actinopterygii) based on transcriptomic and genomic data.
643 *Proceedings of the National Academy of Sciences of the USA* 115: 6249-6254.
644 <https://doi.org/10.1073/pnas.1719358115>
- 645
646 Janssen, J., & Harbison, G.R. 1981. Fish in salps: the association of squaretails
647 (*Tetragonurus* spp.) with pelagic tunicates. *Journal of the Marine Biological Association of*
648 *the United Kingdom*. 61: 917-927. <https://doi.org/10.1017/S0025315400023055>
- 649
650 Johnson, G.D. 1993. Percomorph phylogeny: progress and problems. *Bulletin of Marine*
651 *Science* 52: 3-28.
- 652

Formatted: Font: Italic

653 Katoh, K., Misawa, K., Kuma, K., & Miyata, T. 2002. MAFFT: a novel method for rapid
654 multiple sequence alignment based on fast Fourier transform. *Nucleic Acids Research* 30:
655 3059–3066. <https://doi.org/10.1093/nar/gkf436>
656
657 Katoh, K., & Standley, D.M. 2013. MAFFT Multiple Sequence Alignment Software
658 Version 7: Improvements in Performance and Usability. *Molecular Biology and Evolution*
659 30: 772–780. <https://doi.org/10.1093/molbev/mst010>
660
661 Lanfear, R., Calcott, B., Kainer, D., Mayer, C., & Stamatakis, A. 2014. Selecting optimal
662 partitioning schemes for phylogenomic datasets. *BMC Evolutionary Biology*, 14(1), 82.
663 <https://doi.org/10.1186/1471-2148-14-82>
664
665 Lanfear, R., Frandsen, P. B., Wright, A. M., Senfeld, T., & Calcott, B. 2016.
666 PartitionFinder 2: new methods for selecting partitioned models of evolution for molecular
667 and morphological phylogenetic analyses. *Molecular Biology and Evolution* 34: 772-773.
668 <https://doi.org/10.1093/molbev/msw260>
669
670 Li, H., & Durbin, R., 2009. Fast and accurate short read alignment with Burrows–Wheeler
671 transform. *Bioinformatics* 25, 1754–1760. <https://doi.org/10.1093/bioinformatics/btp324>
672
673 Li, H., Handsaker, B., Wysoker, A., Fennell, T., Ruan, J., Homer, N., Marth, G., Abecasis,
674 G., Durbin, R., & 1000 Genome Project Data Processing Subgroup. 2009. The sequence
675 alignment/map format and SAMtools. *Bioinformatics* 25, 2078–2079.
676 <https://doi.org/10.1093/bioinformatics/btp352>
677
678 Mansueti, R. 1963. Symbiotic behavior between small fishes and jellyfishes, with new data
679 on that between the stromateid, *Peprilus alepidotus*, and the *Scyphomedusa*, *Chrysaora*
680 *quinquecirrha*. *Copeia* 1963: 40-80. <https://doi.org/10.2307/1441273>.
681

Formatted: Font: Italic

Formatted: Font: Italic

Formatted: Font: Italic

Formatted: Font: Italic

- 682 Miya, M., Friedman, M., Satoh, T.O., Takeshima, H., Sado, T., Iwasaki, W., Yamanoue,
683 Y., Nakatani, M., Mabuchi, K., Inoue, J.G., Poulsen, J.Y., Fukunaga, T., Sato, Y., &
684 Nishida, M. 2013. Evolutionary origin of the Scombridae (tunas and mackerels): members
685 of a Paleogene adaptive radiation with 14 other pelagic fish families. *PLoS ONE* 8, e73535.
686 <https://doi.org/10.1371/journal.pone.0073535>
687
- 688 Near, T.J., Dornburg, A., Eytan, R.I., Keck, B.P., Smith, W.L., Kuhn, K.L., Moore, J.A.,
689 Price, S.A., Burbink, F.T., Friedman, M., & Wainwright, P.C. 2013. Phylogeny and tempo
690 of diversification in the superradiation of spiny-rayed fishes. *Proceedings of the National*
691 *Academy of Sciences of the USA* 110: 12738-12743.
692 <https://doi.org/10.1073/pnas.1304661110>
693
- 694 Nelson, J.S., Grande, T.C., & Wilson, M.V.H. 2016. *Fishes of the World*. 5th Edition, John
695 Wiley and Sons, Hoboken, New Jersey. <https://doi.org/10.1002/9781119174844>
696
- 697 Nguyen, L.T., Schmidt, H.A., von Haeseler, A., & Minh, B.Q. 2015. IQ-TREE: A fast and
698 effective stochastic algorithm for estimating maximum likelihood phylogenies. *Molecular*
699 *Biology and Evolution* 32: 268-274. <https://doi.org/10.1093/molbev/msu300>
700
- 701 Rambaut A, Drummond, A.J., Xie, D., Baele, G., & Suchard, M.A. 2018. Posterior
702 summarisation in Bayesian phylogenetics using Tracer 1.7. *Systematic Biology* 67: 901-
703 904. <https://doi.org/10.1093/sysbio/syy032>
704
- 705 Ronquist, F., Teslenko, M., Van Der Mark, P., Ayers, D.L., Darling, A., Höhna, S., Larget,
706 B., Liu, L., Suchard, M.A., & Huelsenbeck, J.P. 2012. MrBayes 3.2: efficient Bayesian
707 phylogenetic inference and model choice across a large model space. *Systematic Biology*
708 61: 539-542. <https://doi.org/10.1093/sysbio/sys029>
709
- 710 Smith, S.A., Moore, M.J., Brown, J.W., & Yang, Y. 2015. Analysis of phylogenomic
711 datasets reveals conflict, concordance, and gene duplications with examples from animals

712 and plants. *BMC Evolutionary Biology*. 15: 150. [https://doi.org/10.1186/s12862-015-0423-](https://doi.org/10.1186/s12862-015-0423-0)
713 0
714
715 Smith, W.L., Craig, M.T., & Quattro, J.M. 2007. Casting the percomorph net broadly: the
716 importance of broad taxonomic sampling in the search for placement of the Serranid and
717 percid fishes. *Copeia* 2007: 35-55. [https://doi.org/10.1643/0045-](https://doi.org/10.1643/0045-8511(2007)7[35:CTPNWT]2.0.CO;2)
718 8511(2007)7[35:CTPNWT]2.0.CO;2
719
720 Thacker, C.E., Satoh, T.P., Katayama, E., Harrington, R.C., Eytan, R.I., & Near, T.J. 2015.
721 Molecular phylogeny of Percomorpha resolves *Trichonotus* as sister to Gobioidae
722 (Teleostei: Gobiiformes) and confirms the polyphyly of Trachinoidei. *Molecular*
723 *Phylogenetics and Evolution* 93: 172-179. <https://doi.org/10.1016/j.ympev.2015.08.001>
724
725 Walker, J.F., Brown, J.W., & Smith, S.A. 2018. Analyzing contentious relationships and
726 outlier genes in phylogenomics. *Systematic Biology* 67: 916-924.
727 <https://doi.org/10.1093/sysbio/syy043>
728
729 Yagashita, N., Miya, M., Yamanoue, Y., Shirai, S.M., Nakayama, K., Suzuki, N., Satoh,
730 T.P., Mabuchi, K., Nishida, M., & Nakabo, T. 2009. Mitogenomic evaluation of the unique
731 facial nerve pattern as a phylogenetic marker within the perciform fishes (Teleostei:
732 Percomorpha). *Molecular Phylogenetics and Evolution* 53: 258-266.
733 <https://doi.org/10.1016/j.ympev.2009.06.009>
734
735 Zhang, C., Rabiee, M., Sayyari, E., & Mirarab, S. 2018. ASTRAL-III: Polynomial Time
736 Species Tree Reconstruction from Partially Resolved Gene Trees. *BMC Bioinformatics* 19:
737 153. <https://doi.org/10.1186/s12859-018-2129-y>
738
739
740
741

Formatted: Font: Italic

742 **Figure Legends**

743
744 Figure 1. *Amarsipus carlsbergi*, photographed on 7 February 2019, Romblon, Phillipines.
745 Photograph provided by courtesy of Linda Ianniello.

746
747 Figure 2. Previous phylogenetic hypotheses of *Amarsipus carlsbergi*. (A) Horn, 1984,
748 topology inferred from cladistic analysis of 27 morphological traits; (B) Doiuchi et al.,
749 2004, topology inferred from 36 morphological traits; (C) Campbell et al., 2018, topology
750 inferred from analysis of 10 genetic loci.

751
752 Figure 3. A-B. Phylogeny of Pelagiaria inferred by analysis of 610 concatenated,
753 partitioned UCE loci in Exabayes and IQTree. (A) Phylogenetic tree with branch lengths
754 drawn relative to number of substitutions; (B) Same tree as in A, but with ultrametric
755 branch length transformation and annotated to illustrate Bayesian and Maximum
756 Likelihood node support. Support values are shown adjacent to each node, with ExaBayes
757 Bayesian posterior probability (BPP) first, followed by IQTree maximum likelihood
758 bootstrap support (BS). Nodes with both maximum BPP and BS support are indicated with
759 an asterisk. *Amarsipus* is highlighted in yellow, and stromateoid families bearing a
760 pharyngeal sac are highlighted in blue.

761
762 Figure 4. A-C. Topologies inferred from concatenation and species tree analyses annotated
763 with node support, concordance factors, and number of loci strongly supporting each
764 node. (A) IQTree analysis of partitioned, concatenated UCE loci; (B) ASTRAL-III species
765 tree analysis conducted without node-support filtering; (C) ASTRAL-III species tree
766 conducted with gene trees for which nodes that have lower than 15% bootstrap support are
767 collapsed. Support values are indicated with colored discs on nodes, with black
768 representing 95-100% bootstrap support (BS) for IQTree or 0.95-1.0 Local Posterior
769 Probability (LPP); gray indicating 80-95% BS or 0.8-0.95 LPP; and white representing
770 nodes with support values lower than 80% BS or 0.8 LPP. BUCKy-estimated concordance

Deleted: ¶

Deleted: ,

Deleted: provided

Deleted: partitioned,

Deleted: 610

Deleted: ,

781 factors are indicated above each node, and the percentage of individual UCE loci that
 782 contain partitions corresponding to a node higher than 50% BS are listed below each node.

783

784 Figure 5. A-C. BUCKy concordance factor estimates for the proportion of individual UCE
 785 gene trees in which *Amarsipus* (A), *Tetragonurus* (B), and Chiasmodontidae (C) appear in
 786 topological partitions with each Pelagiarian family.

787

788

789

790 Tables

791

792 Table 1. Proportions of UCE loci supporting alternative relationships between *Amarsipus*,
 793 *Tetragonurus*, and Chiasmodontidae. Sample-wide concordance factors represent the
 794 proportion of loci for which the partition was estimated to be the true topology, as
 795 estimated in BUCKy with MrBayes-inferred gene tree distributions. The proportion of loci
 796 exceeding either a 50% or 80% bootstrap support threshold were estimated using IQTree-
 797 inferred gene trees for each UCE locus.

| | <i>Amarsipus</i> - <i>Tetragonurus</i> | <i>Amarsipus</i> - Chiasmodontidae | <i>Tetragonurus</i> - Chiasmodontidae |
|---------------------------------|---|---------------------------------------|--|
| Sample-wide concordance factor | 0.201 | 0.194 | 0.255 |
| Proportion of loci with > 50 BS | 0.007 | 0.007 | 0.149 |
| Proportion of loci with > 80 BS | 0.002 | 0.003 | 0.062 |

798

799

800

801

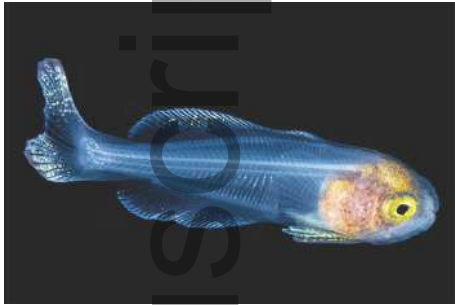
802

803

804

805

806 Figure 1.

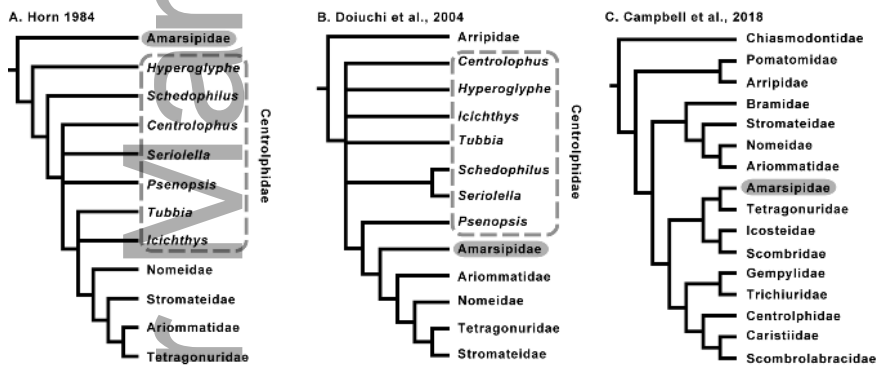


807

808

809

810 Figure 2.



811

812

813

814

815

816

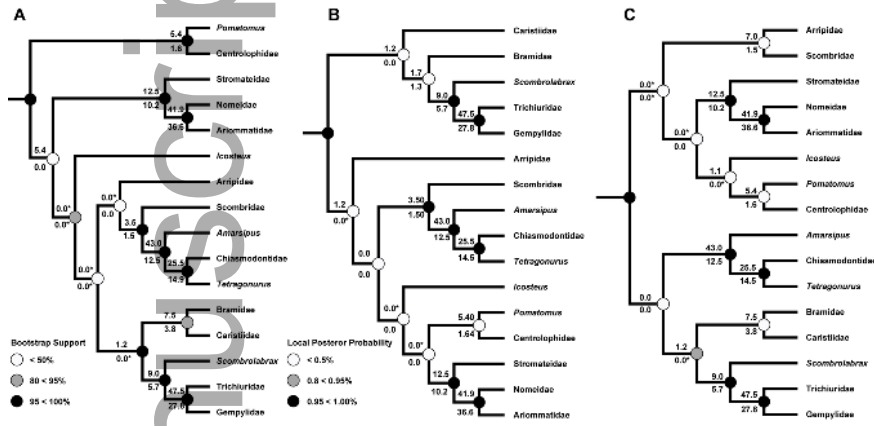
817

818

819

820

826 Figure 4.

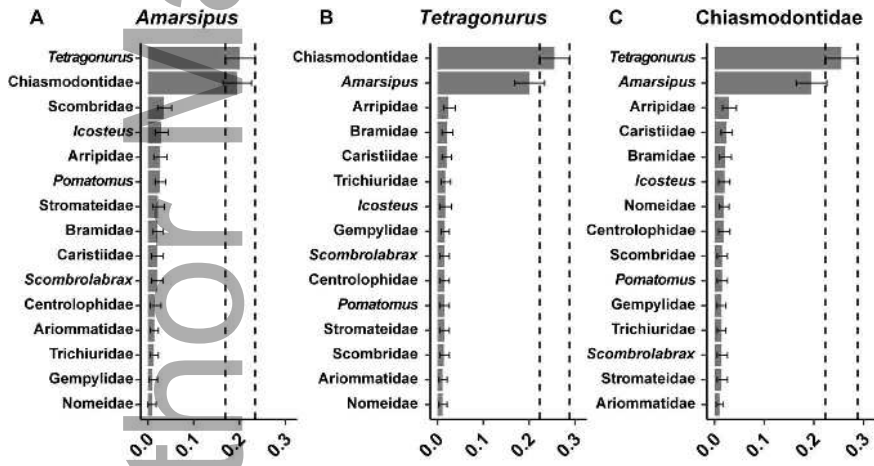


827

828

829

830 Figure 5.



831